Scilight

Urban and Building Science
https://www.sciltp.com/journals/ubs



Article

Check for updates

An Adaptive Radiative Cooling Roof Panel Approach for Balancing Building Cooling Benefits and Heating Penalties

Yang Hu [1,*], Baoshuang Zhu [1], Yujie Zhang [2,3] and Weixian Mu [4,*]

[1] School of Civil Engineering, Southeast University, Nanjing 211189, China
[2] Department of Civil Engineering, School of Engineering, Monash University Malaysia, Jalan Lagoon Selatan, Bandar Sunway, Subang Jaya 47500, Selangor, Malaysia
[3] Department of Civil Engineering, Monash University, Clayton, VIC 3800, Australia
[4] Department of Architecture, Built Environment and Construction, Politecnico di Milano, 20133 Milano, Italy
* Correspondence: 230248199@seu.edu.cn (Y.H.); weixian.mu@polimi.it (W.M.)

How To Cite: Hu, Y.; Zhu, B.; Zhang, Y.; et al. An Adaptive Radiative Cooling Roof Panel Approach for Balancing Building Cooling Benefits and Heating Penalties. *Urban and Building Science* **2026**. https://doi.org/10.53941/ubs.2026.100025

Received: 14 July 2026
Revised: 6 August 2026
Accepted: 17 August 2026
Published: 21 August 2026

Abstract: Radiative cooling (RC) roofs can reduce cooling energy use but may impose heating penalties in climates with cold seasons. This study evaluates an adaptive RC roof panel deployed only during cooling-dominated months to provide effective building cooling and energy savings under hot conditions while avoiding heating penalties under cold conditions. A transient multi-node model was used to couple heat transfer among the panel, roof, and indoor air, with hourly ERA5 data serving as boundary conditions. Nanjing was examined in detail, followed by a cross-climate assessment of nine additional Chinese cities. For Nanjing, baseline annual HVAC electricity use was 2763.8 kWh, of which 65.2% was attributable to cooling. A fixed panel reduced annual HVAC electricity use by 24.0%, whereas monthly adaptive deployment increased annual savings to 30.7% by preserving cooling-season benefits while avoiding most winter heating penalties. The panel coverage ratio exerted a substantially stronger influence than the panel-to-roof gap. Across cities, the adaptive strategy provided the greatest incremental benefit over fixed installation in colder climates, with additional annual savings of 343.85 kWh in Harbin, 331.02 kWh in Urumqi, 289.23 kWh in Beijing, and 266.82 kWh in Yinchuan. By contrast, this advantage diminished in cooling-dominated climates and became negligible in Guangzhou and Haikou. These findings indicate that RC roofs should be evaluated as seasonally controlled building-envelope systems rather than static surfaces, particularly where both heating and cooling demands are substantial.

Keywords: radiative cooling; adaptive roof; energy consumption; climate-responsive

1. Introduction

Building cooling demand driven by extreme heat and the urban heat island effect poses a major challenge to the transition toward low-carbon cities [1–3]. This challenge is intensified by urbanization, rising outdoor temperatures, and more frequent extreme heat events, which jointly increase cooling demand and peak electricity loads. Although active cooling approaches can provide effective cooling, they usually require additional energy input or mechanical equipment, thereby increasing building loads and hindering low-carbon and sustainable cooling [4–6]. Consequently, passive cooling strategies for building envelopes are becoming increasingly important for reducing heat gains to building interiors and dependence on mechanical air-conditioning systems during cooling-dominated seasons [7–9]. Radiative cooling (RC) has emerged as a promising passive cooling approach for buildings. It reduces solar heat absorption while enhancing long-wave thermal emission through the mid-infrared atmospheric window, thereby allowing terrestrial surfaces to dissipate heat to cold outer space without external energy input [10–13]. Since the experimental demonstration of sub-ambient daytime RC under

Copyright: © 2026 by the authors. This is an open access article under the terms and conditions of the Creative Commons Attribution (CC BY) license (https://creativecommons.org/licenses/by/4.0/).
Publisher's Note: Scilight stays neutral with regard to jurisdictional claims in published maps and institutional affiliations.

direct sunlight, considerable progress has been made in photonic structures, polymer coatings, porous films, paints, structural materials, and RC heat exchangers [14–17]. These studies have shown that RC materials can lower roof or surface temperatures, reduce cooling loads, and contribute to urban heat mitigation [18–21]. RC therefore represents a promising building-envelope strategy for reducing cooling-related energy demand.

However, despite the considerable potential of RC for urban building applications, excessive cooling under cold-climate conditions may increase heating demand, which remains a major challenge limiting widespread adoption. Most existing building applications of RC use fixed coatings, membranes, paints, or roof-integrated surfaces with static optical and radiative properties [19,22,23]. This approach is simple and feasible but subject to seasonal performance limitations. The high cooling potential enabled by high solar reflectance and high infrared emissivity can effectively reduce indoor heat gain under high-temperature and high-radiation conditions. However, this passive and continuously operating cooling mechanism may introduce an additional heating penalty under cold conditions. Therefore, fixed RC roofs face an inherent challenge in balancing cooling-load reductions against heating penalties. This challenge is particularly pronounced for buildings in mixed-climate regions with substantial cooling and heating demands, where the heating penalty may be amplified and even become dominant [24–27]. Researchers have developed dynamic and dual-mode thermal regulation systems to improve the year-round energy performance of static cooling surfaces. These systems include temperature-sensitive coatings, thermochromic windows, switchable RC systems, and integrated RC-solar heating devices [28–30]. However, many of these systems rely on intrinsic property changes, fixed transition temperatures, or complex material structures [31]. They typically require more complex fabrication processes and incur higher costs, while their long-term stability remains to be validated [32,33].

Here, we propose a potentially viable strategy that decouples RC from the roof, allowing energy exchange among the panel, roof, and environment to be controlled for greater overall energy savings. When cooling is required, the RC surface is deployed above the conventional roof surface, reflects most incident solar radiation, and dissipates heat passively through the atmospheric window. When heating demand becomes dominant, the RC surface is removed to prevent excessive cooling and the resulting heating penalty. However, this approach to thermal-coupling control has received relatively limited attention. Although related concepts based on controllable thermal contact or thermal-resistance modulation have been reported [33,34], their integration into roof assemblies and their performance under realistic year-round operating conditions remain insufficiently investigated.

Can adaptive RC roofs reduce cooling demand while avoiding additional heating penalties across different climatic conditions? To address this question, this study proposes an adaptive RC panel installed above the building roof. In contrast to conventional RC coatings that are permanently attached to the building envelope, this approach allows the panel to be selectively installed or removed according to monthly heating and cooling requirements. A transient thermodynamic model was employed to account for combined heat transfer among the RC panel, roof, and indoor air. Hourly ERA5 data served as the meteorological boundary conditions. Nanjing was selected as the primary case-study city for detailed analysis of monthly energy demand, typical-day free-floating indoor temperature, and the effects of panel coverage ratio and panel-to-roof gap. The analysis was then extended to representative Chinese cities to assess the suitability of fixed and adaptive RC configurations across different climates. This work shifts the assessment of RC roofs from a traditional static, cooling-material perspective to a seasonally adaptive, building-energy perspective. The proposed adaptive panel is not intended to provide maximum cooling at all times; instead, it is intended to align RC operation with seasonal building thermal requirements. This approach offers a more stable basis for applying RC roofs in regions with both cooling and heating demands and provides a climate-responsive design framework for large-scale deployment of RC technology.

2. Methodology

2.1. Research Design and Roof Configurations

This study evaluates the thermal and energy performance of a movable RC panel installed above a building roof. The panel is designed to reduce solar heat gain and enhance radiative heat rejection during cooling-dominated periods and is removed during heating-dominated periods to avoid additional heating penalties. A transient building-roof-panel model was developed to quantify the coupled effects of solar reflection, long-wave radiation, convective heat transfer, roof heat storage, indoor thermal inertia, and HVAC energy demand.

Three roof configurations were compared:

1. Baseline roof: the roof is directly exposed to the outdoor environment without an RC panel.
2. Fixed panel: the RC panel is installed throughout the year.
3. Adaptive panel: the RC panel is installed or removed on a monthly basis according to the cooling and heating demands of the baseline roof.

The three-dimensional schematic of the building model and the energy flow diagrams with and without the RC panel are shown in Figure 1.

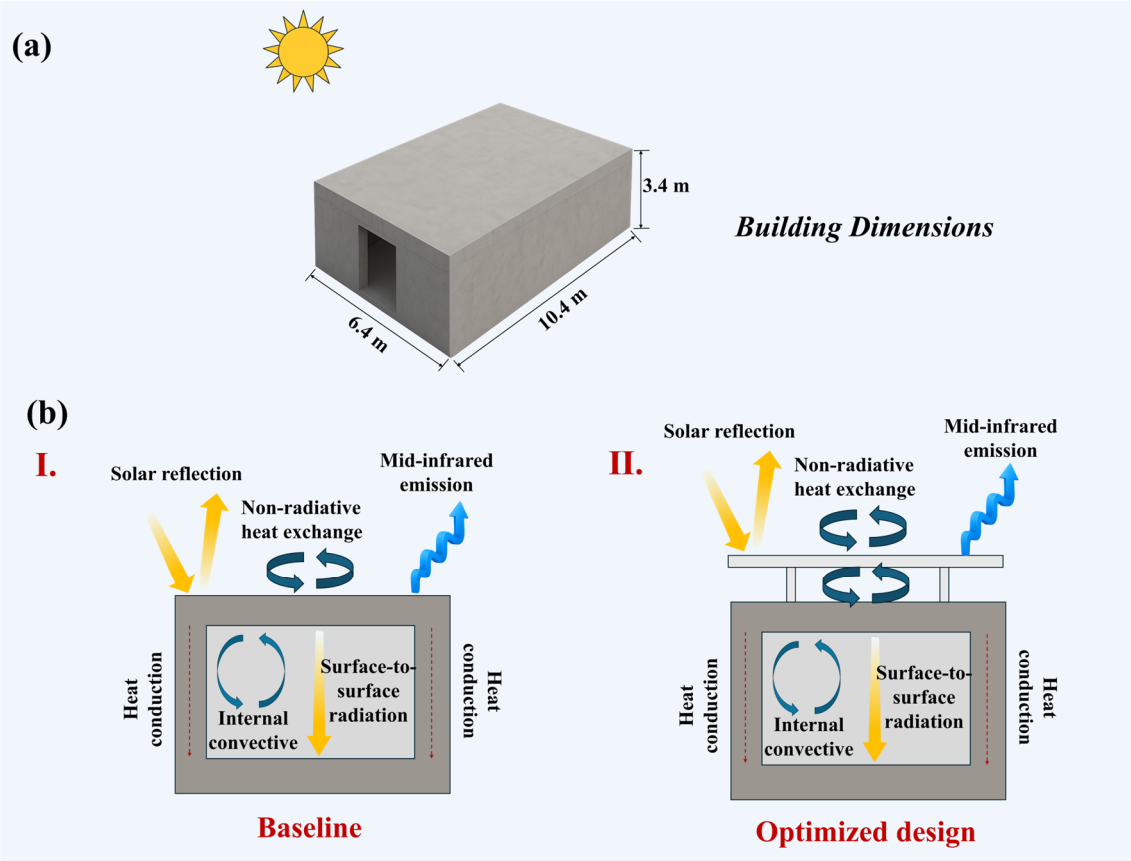


Figure 1. (**a**) Three-dimensional schematic of the building model and (**b**) energy-flow diagrams for roof configurations with and without the RC panel.

2.2. Meteorological Data and City Selection

Hourly meteorological data were obtained from ERA5 [35]. The variables used in the model were 2-m air temperature, 10-m wind speed, and surface solar radiation for 2018. The data were stored as monthly NetCDF files. For each city, the hourly meteorological series were extracted from the grid point nearest to the corresponding city coordinates.

Environmental parameters for the thermal model were ambient air temperature (T_{amb}), wind speed (v), and solar irradiance (G).

Nanjing was selected for detailed analysis because it lies in the hot-summer and cold-winter climate zone, where both cooling and heating demands are relevant. To further evaluate regional applicability, the model was also applied to representative Chinese cities, including Harbin, Urumqi, Yinchuan, Beijing, Nanjing, Wuhan, Changsha, Kunming, Guangzhou, and Haikou.

2.3. Transient Thermodynamic Analysis

The transient thermal response of the roof-panel-indoor system was represented using a multi-node model developed as an optimized version of a previously validated finite element model, with its fundamental parameters obtained from previous research [36]. Specifically, a numerical solution was obtained using a COMSOL-based model for the baseline roof configuration, while an analytical solution was derived from the transient energy-balance equations. Model accuracy was validated by comparing the interpolated roof and indoor air temperatures obtained using the two methods on 1 May 2025. The mean squared error (MSE) and root mean squared error (RMSE) indicated good agreement between the numerical and analytical solutions, as shown in Figure 2.

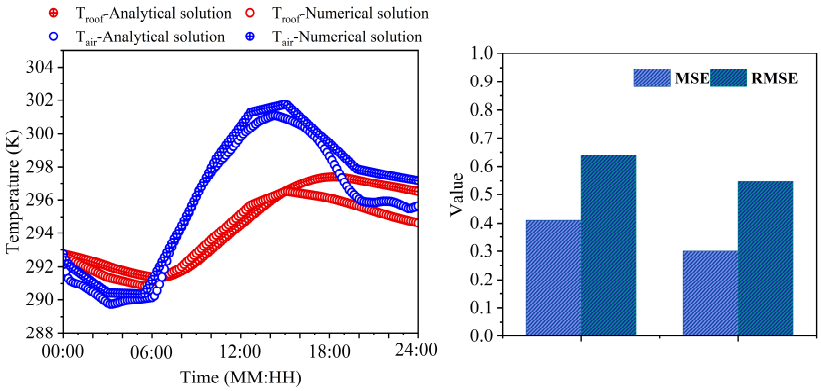


Figure 2. Comparison of roof and indoor air temperatures obtained from the analytical and COMSOL-based numerical models on May 1 May 2025.

The transient thermodynamic model was solved using a fourth-order Runge-Kutta (RK4) time integration scheme with a 1 h time step over a complete annual simulation (8760 h). The initial temperatures of the panel, roof, indoor air, and internal thermal mass were set equal to the ambient temperature during the first hour of the meteorological dataset. Because the solution at each time step was obtained explicitly without an iterative nonlinear solver, no additional convergence criterion was required. The indoor thermal capacity was represented by an equivalent air capacitance together with an internal thermal mass coupled to the indoor air through a convective heat transfer coefficient, allowing the model to account for building thermal inertia. Heat transfer between the indoor space and the outdoor environment included conduction through opaque walls and windows, window solar heat gains, and air exchange with an infiltration rate of 0.5 h^{-1}. External convection was calculated using a wind-dependent heat transfer coefficient. The air gap between the radiative cooling (RC) panel and the roof was treated as an enclosed air cavity. The convective heat transfer coefficient within the cavity, h_{gap}, was assumed to be constant at 2.5 W m^{-2} K^{-1}. The HVAC system was represented by an ideal setpoint controller that operated whenever the predicted indoor temperature exceeded 299 K or fell below 293 K, corresponding to the cooling and heating setpoints, respectively. To focus on the influence of the roof RC strategy, internal gains from occupants, lighting, and plug loads were represented by an equivalent thermal mass.

The transient energy balance was expressed as:

$$C_i \frac{dT_i}{dt} = \sum Q_i \tag{1}$$

where C_i is the equivalent heat capacity of node (i), T_i is the node temperature, and ΣQ_i is the net heat flow rate into the node.

The effective sky temperature T_{sky} (K) was calculated using an empirical relation based on T_{amb} (K) [37]:

$$T_{sky} = 0.037536 T_{amb}^{1.5} + 0.32 T_{amb} \tag{2}$$

2.4. Baseline Roof Energy Balance

For the baseline roof, the external roof surface exchanges heat with solar radiation, outdoor air, the sky, and the indoor space. The solar heat gain absorbed by the roof is:

$$Q_{roof,sol} = \alpha_{roof} G A_{roof} \tag{3}$$

where α_{roof} is the roof solar absorptance and A_{roof} (m^2) is the roof area. In this study, the solar reflectance of the baseline roof was 0.15 [38]; therefore, the corresponding solar absorptance was 0.85.

The convective heat exchange between the roof and ambient air was calculated as:

$$Q_{roof,conv} = h_{ext} A_{roof} \left(T_{roof} - T_{amb}\right) \tag{4}$$

where h_{ext} (W m^{-2} K^{-1}) is the external convective heat transfer coefficient. It was estimated from wind speed as [39]:

$$h_{ext} = 5.7 + 3.8v \tag{5}$$

The long-wave radiative heat exchange between the roof and the sky was calculated as:

$$Q_{roof,sky} = \varepsilon_{roof}\sigma A_{roof}(T_{roof}^4 - T_{sky}^4) \quad (6)$$

where ε_{roof} is the roof emissivity and σ is the Stefan-Boltzmann constant. T_{roof} and T_{sky} are the roof and sky temperatures, respectively.

The heat transferred from the roof to the indoor air was represented by an equivalent conductance:

$$Q_{roof-air} = G_{roof-air}(T_{roof} - T_{air}) \quad (7)$$

where $G_{roof\text{-}air}$ (W K^{-1}) includes heat conduction through the roof and convection at the indoor roof surface.

Roof thermal properties are shown in Table 1.

Table 1. Roof thermal properties.

Parameter	Value	Unit
Roof specific heat capacity	837.4	J kg^{-1} K^{-1}
Thickness	0.150	m
Density	1930.0	kg m^{-3}
Roof thermal conductivity	1.69	W m^{-1} K^{-1}
Interior roof convective heat-transfer coefficient	3.0	W m^{-2} K^{-1}

2.5. Adaptive RC Panel Model

When the RC panel is installed, the panel is positioned above the roof with a prescribed air gap. The panel reflects most incident solar radiation and releases heat to the sky through long-wave radiation. The solar reflectance and long-wave emissivity of the panel were set to 0.95 and 0.96, respectively [40]. Therefore, the solar radiation absorbed by the panel is:

$$\alpha_{panel} = 1 - \rho_{panel} \quad (8)$$

$$Q_{panel,sol} = \alpha_{panel} G A_{panel} \quad (9)$$

where A_{panel} (m^2) is the panel area.

The convective heat exchange between the panel and outdoor air is:

$$Q_{panel,amb} = h_{ext} A_{panel}(T_{panel} - T_{amb}) \quad (10)$$

The long-wave radiative heat exchange between the panel and the sky is:

$$Q_{panel,sky} = \varepsilon_{panel}\sigma A_{panel}(T_{panel}^4 - T_{sky}^4) \quad (11)$$

The panel also exchanges heat with the roof through convection and long-wave radiation across the panel–roof gap. The convective heat exchange between the panel and the roof is:

$$Q_{panel-roof,conv} = h_{gap} A_{panel}(T_{panel} - T_{roof}) \quad (12)$$

where h_{gap} (W m^{-2} K^{-1}) is the equivalent heat transfer coefficient within the gap; this value was set to 2.5. When the gap is zero, the panel-to-roof interaction is treated as contact or near-contact heat transfer.

The long-wave radiative exchange between the panel and roof is:

$$Q_{panel-roof,rad} = \varepsilon_{eff}\sigma A_{panel}(T_{panel}^4 - T_{roof}^4) \quad (13)$$

where the effective emissivity between the two facing surfaces is:

$$\varepsilon_{eff} = \frac{1}{\frac{1}{\varepsilon_{panel}} + \frac{1}{\varepsilon_{roof}} - 1} \quad (14)$$

When the panel does not fully cover the roof, the uncovered area remains directly exposed to solar radiation, ambient air, and the sky. This uncovered area was treated using the same energy balance as the baseline roof.

Thermal properties of the radiative cooling panel are shown in Table 2.

Table 2. Thermal properties of the radiative cooling panel.

Parameter	Value	Unit
Specific heat capacity	1010.0	J kg^{-1} K^{-1}
Thickness	0.050	m
Density	3455	kg m^{-3}

2.6. Indoor Air and Thermal Mass Balance

The indoor air node receives heat from the roof, the building envelope, air exchange, window solar gain, and indoor thermal mass. Its energy balance is:

$$C_{air}\frac{dT_{air}}{dt} = Q_{roof-air} + Q_{env-air} + Q_{win,sol} + Q_{mass-air} \quad (15)$$

where $C_{air} = 2.17 \times 10^5$ J K^{-1} is the equivalent indoor air heat capacity [41]. To highlight roof-dominated variations in building heating and cooling loads, the parameters and calculations associated with the building facades were simplified consistently.

The heat exchange between indoor air and the outdoor environment through walls, windows, and air exchange is:

$$Q_{env-air} = (G_{env} + G_{vent})(T_{amb} - T_{air}) \quad (16)$$

where G_{env} = 106.2 W K^{-1} is the equivalent envelope conductance and G_{vent} (W K^{-1}) is the equivalent ventilation or infiltration conductance.

The window solar heat gain is calculated as:

$$Q_{win,sol} = SHGC \cdot G \cdot A_{win} \cdot F_{win} \quad (17)$$

where $SHGC$ = 0.45 is the solar heat gain coefficient [42], A_{win} = 27 m^2 is the window area, and F_{win} = 0.25 is an equivalent solar gain reduction factor accounting for building orientation, external shading, and the effective solar exposure of the window.

The heat exchange between indoor air and indoor thermal mass is:

$$C_{mass}\frac{dT_{mass}}{dt} = -Q_{mass-air} \quad (18)$$

Indoor air and ventilation parameters are shown in Table 3.

Table 3. Indoor air and ventilation parameters.

Parameter	Value	Unit
Specific heat capacity of air	1008.0	J kg^{-1} K^{-1}
Air density	1.2	kg m^{-3}
Air change rate	0.5	h^{-1}
Ventilation thermal conductance	30.2	W K^{-1}

Wall and window heat transfer parameters are shown in Table 4.

Table 4. Wall and window heat transfer parameters.

Parameter	Value	Unit
Exterior wall U-value	0.6	W m^{-2} K^{-1}
Window U-value	2.4	W m^{-2} K^{-1}

2.7. HVAC Energy Demand Calculation

The HVAC energy demand was calculated using an ideal setpoint control approach. For each time step, the indoor air temperature was first predicted from the transient energy balance under free-running conditions. The predicted temperature was then compared with the cooling and heating setpoints. Cooling or heating energy was supplied only when the predicted temperature exceeded the cooling setpoint or fell below the heating setpoint, respectively, and the corresponding load was determined from the energy required to restore the indoor temperature to the prescribed setpoint.

The cooling and heating setpoints were 299 K and 293 K, respectively [43]. The hourly cooling load was calculated as:

$$Q_{cool} = C_{air}\left(T_{air,free} - T_{cool}\right),\ T_{air,free} > T_{cool} \tag{19}$$

and the hourly heating load was calculated as:

$$Q_{heat} = C_{air}\left(T_{heat} - T_{air,free}\right),\ T_{air,free} < T_{heat} \tag{20}$$

where $T_{air,free}$ (K) is the predicted indoor air temperature before HVAC correction, T_{cool} (K) is the cooling setpoint, and T_{heat} (K) is the heating setpoint.

The thermal loads were converted to electricity consumption using the cooling and heating coefficients of performance:

$$E_{cool} = \frac{Q_{cool}}{COP_{cool}}\ E_{heat} = \frac{Q_{heat}}{COP_{heat}} \tag{21}$$

where COP_{heat} = 3.0 and COP_{cool} = 3.2 [44].

Monthly and annual cooling, heating, and total HVAC electricity consumption were then obtained for each roof configuration.

2.8. Free-Floating Indoor Temperature Simulation

In addition to the HVAC-controlled simulation, a free-floating indoor temperature simulation was performed for Nanjing. In this simulation, no heating or cooling correction was applied to the indoor air node. Therefore, the indoor temperature was allowed to evolve naturally according to the transient heat balance.

The free-floating simulation was used to evaluate the passive effect of the RC panel on the indoor thermal environment. It was not used to calculate HVAC energy consumption. This separation is important because the HVAC-controlled simulation quantifies the energy required to maintain comfort setpoints, whereas the free-floating simulation shows the natural variation in indoor temperature without active conditioning.

For Nanjing, hourly free-floating indoor temperatures were calculated for the baseline roof, fixed panel, and adaptive panel configurations.

2.9. Selective Installation Method

The adaptive configuration was controlled using a monthly deployment rule. First, the baseline-roof case was simulated for the full year. Monthly cooling electricity demand ($E_{cool,m}$) and heating electricity demand ($E_{heat,m}$) were then calculated from this baseline. The panel was installed when cooling demand exceeded heating demand and removed otherwise, as summarized in Figure 3.

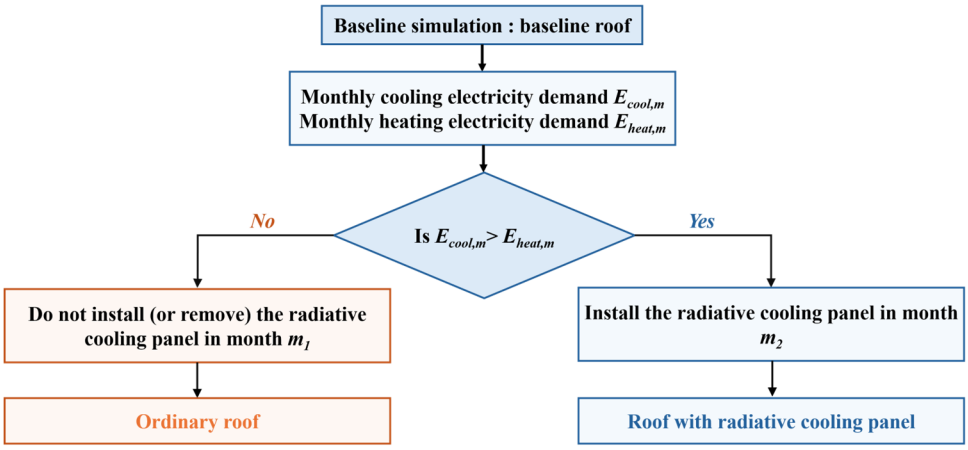


Figure 3. Monthly deployment rule for the RC panel.

For month m, the RC panel is installed when:

$$E_{cool,m} > E_{heat,m} \tag{22}$$

and removed when:

$$E_{cool,m} \leq E_{heat,m} \tag{23}$$

During heating-dominated months, the panel is removed to reduce the risk of additional heat loss and an associated heating-energy penalty.

2.10. Applicability Assessment for Representative Cities

Analysis across different climatic conditions can help determine where the adaptive roof is most suitable and how widely it can be applied. Consequently, the same model was applied to representative Chinese cities. For each city, hourly ERA5 meteorological data from the nearest grid point were used as boundary conditions. The baseline roof, fixed panel, and adaptive panel configurations were simulated using the same building and panel parameters.

For each city and roof configuration, monthly and annual cooling, heating, and total HVAC electricity consumption were calculated. Adaptive deployment months were identified from the baseline monthly cooling and heating demands. The cross-city comparison was used to identify the climatic conditions under which movable deployment provides a meaningful advantage over fixed installation.

3. Results

3.1. Baseline Heating and Cooling Loads of the Reference Building in Nanjing

The energy-saving performance of RC varies throughout the year, highlighting the importance of evaluating RC performance on a monthly basis. RC roofs provide the greatest benefits when reduced roof heat gains lead to lower cooling demand, but they may increase heating demand by limiting beneficial solar heat gains during cold periods. Their applicability should therefore be assessed on the basis of both annual net energy consumption and the monthly balance between cooling and heating demands [45]. To provide a baseline for this assessment, the monthly HVAC electricity consumption of the baseline-roof case in Nanjing was first analyzed.

Figure 4 shows the monthly HVAC electricity consumption of the baseline-roof case in Nanjing. The annual consumption was 2763.8 kWh, comprising 1801.7 kWh for cooling and 962.1 kWh for heating; cooling therefore accounted for 65.2% of the annual total. Cooling demand was concentrated from May through September and peaked in July at 409.4 kWh, followed by August (375.6 kWh) and June (319.4 kWh), while heating demand occurred primarily from January through March and in December, with the highest monthly value in January (344.7 kWh).

The monthly load distribution supports selective rather than year-round deployment. Cooling demand exceeded heating demand in April and October, whereas March, November, and December remained heating-dominated. For the reference building, the cooling-dominated period therefore extended from April through October. Year-round installation during the remaining months would reduce beneficial winter solar gains and could offset part of the annual cooling benefits.

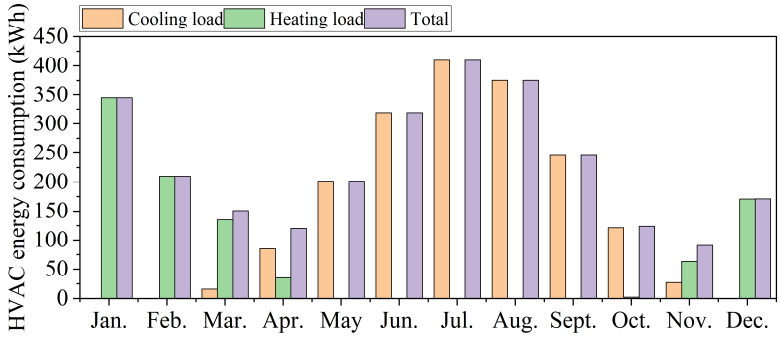


Figure 4. Monthly HVAC electricity consumption of the baseline-roof case in Nanjing.

3.2. Temperature Response Characteristics of the Fixed RC Approach

Because of differences in optical properties, the baseline-roof and RC-roof configurations exhibit distinct time-dependent thermal responses under different weather conditions. Four representative days were selected to evaluate the hourly temperature differences between the two roof configurations. Figure 5 presents hourly meteorological conditions and indoor temperatures for the baseline-roof and fixed-RC-panel configurations on January 1, April 1, July 1, and October 1.

Peak solar irradiance was 145.1 W m^{-2} on January 1, 747.3 W m^{-2} on April 1, 806.5 W m^{-2} on July 1, and 812.1 W m^{-2} on October 1. Ambient temperature ranged from 6.8 to 10.7 °C on January 1 and from 23.7 to 30.9 °C on July 1. On all four days, the indoor temperature peaked after solar noon, reflecting the combined effects of roof heat transfer and indoor thermal storage.

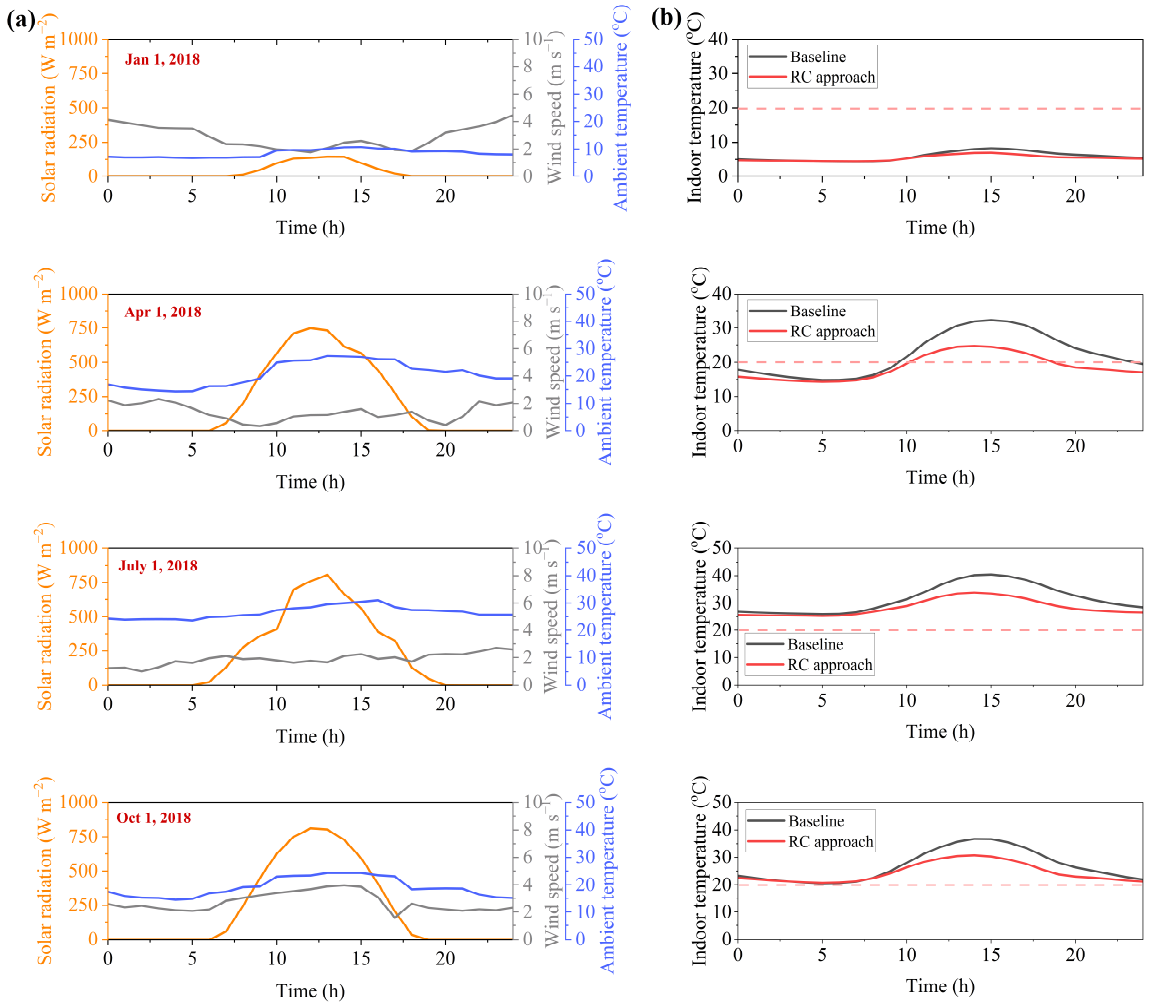


Figure 5. Hourly profiles of (**a**) environmental parameters and (**b**) indoor temperature with and without the RC panel on typical days in Nanjing.

Specifically, the effectiveness of the RC panel depends on the seasonal thermal demand of the building. On January 1, the baseline indoor temperature remained below 20 °C throughout the day, with a maximum value of 8.2 °C. With the RC panel installed, the maximum indoor temperature dropped to 6.9 °C, and the average daily indoor temperature fell by 0.5 °C. Therefore, RC is not suitable for heating-dominated periods because the lower indoor temperature may further increase heating demand.

The RC panel can reduce indoor temperature during summer or under warm climatic conditions. On April 1, the baseline indoor temperature reached 32.4 °C, whereas the maximum temperature in the RC case was limited to 24.7 °C, resulting in a reduction of 7.7 °C. On July 1, under high solar radiation and elevated ambient temperature, the baseline indoor temperature reached 40.4 °C. After applying the RC panel, the peak temperature decreased to 33.7 °C. Although the indoor temperature remained relatively high under free-floating conditions, the maximum temperature reduction reached approximately 6.7 °C, which could reduce cooling demand and the load on the HVAC system. A similar effect was observed on October 1, when the maximum indoor temperature decreased from 36.7 °C to 30.7 °C.

These results support the development of an adaptive installation strategy. The RC panel can reduce indoor temperature during hot and sunny daytime conditions, but its operation is unfavorable during cold periods. Therefore, the RC panel should not be considered a year-round passive measure. It should be applied during the cooling season on the basis of monthly cooling and heating demand characteristics.

3.3. Energy Performance and Advantages of the Adaptive RC Roof

The transient temperature response described above shows that RC is not always energetically beneficial. Under low-temperature conditions, the RC panel further lowers indoor temperature and increases the heating load. This observation indicates that a year-round RC strategy may not be suitable for regions with distinct cold and warm seasons. Therefore, an adaptive RC panel strategy was proposed to mitigate this problem by installing the panel only in cooling-dominated months and removing it during heating-dominated months. Figure 6 shows the monthly cooling, heating, and total HVAC loads of the baseline roof, fixed RC panel, and adaptive RC panel configurations in Nanjing.

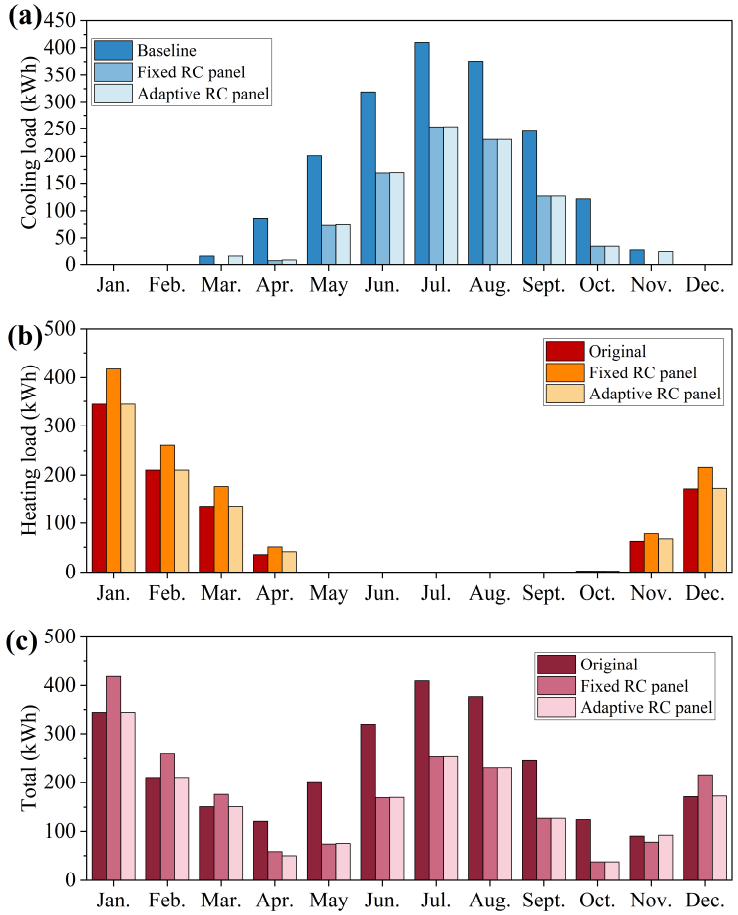


Figure 6. Monthly (**a**) cooling, (**b**) heating, and (**c**) total HVAC electricity consumption for the baseline roof, fixed RC panel, and adaptive RC panel configurations.

As shown in Figure 6a, both RC panel arrangements significantly reduced cooling loads during the cooling period. For the baseline roof, cooling loads in July, August, and June were 409.4 kWh, 375.6 kWh, and 319.4 kWh, respectively. The RC panel reduced these values to approximately 254.0 kWh, 230.9 kWh, and 169.6 kWh, respectively. The fixed and adaptive configurations achieved almost identical cooling-load reductions from April to October because the adaptive strategy deployed the panel during these cooling-dominated months. The fixed panel reduced the annual cooling load from 1801.7 kWh to 896.5 kWh, and the adaptive panel reduced it to 940.4 kWh, corresponding to reductions of 50.2% and 47.8%, respectively.

However, as shown in Figure 6b, the year-round fixed panel caused a clear heating penalty. Relative to the baseline roof, the fixed panel increased heating loads by 73.5 kWh in January, 51.3 kWh in February, and 44.6 kWh in December. The corresponding baseline heating loads were 344.7 kWh, 210.1 kWh, and 170.9 kWh, respectively. The fixed RC panel continued to reflect solar radiation and thus increased heat rejection even when the building required heat gains. In contrast, the adaptive RC panel retained the baseline roof configuration for most of the heating season by removing the panel and thus avoided most of the heating penalty. Its annual heating load was 974.1 kWh, which was only 1.3% higher than that of the baseline roof, whereas the fixed panel increased the annual heating load by 25.0%. The slight increase in the adaptive RC case at the end of autumn and the

beginning of winter was due to carryover thermal effects from the continuous annual simulation, but it was much smaller than that of the fixed configuration.

The overall effect of these changes is shown in Figure 6c. The annual HVAC load of the baseline roof was 2763.8 kWh; after installation of a fixed RC panel, it was reduced to 2099.5 kWh and was further reduced to 1914.5 kWh with the adaptive RC panel. The corresponding total energy savings were 24.0% and 30.7%, respectively. Although the fixed panel achieved a relatively large reduction in cooling load, it also incurred a greater heating penalty in cold weather. By contrast, the adaptive panel had a lower annual HVAC load because it adjusted its operation according to seasonal cooling and heating requirements. Given that Nanjing has a hot-summer and cold-winter climate, the primary purpose of the movable RC panel is to enhance passive cooling while avoiding excessive radiative cooling in winter.

Based on the above comparison, the impact of RC panel design parameters on building energy consumption was further analyzed. The panel coverage ratio determines the proportion of the roof exposed to radiative cooling, and the gap between the panel and the roof surface influences the thermal coupling strength at this interface. Figure 7 shows the annual cooling, heating, and total HVAC loads for different panel coverage ratios and panel-to-roof gaps.

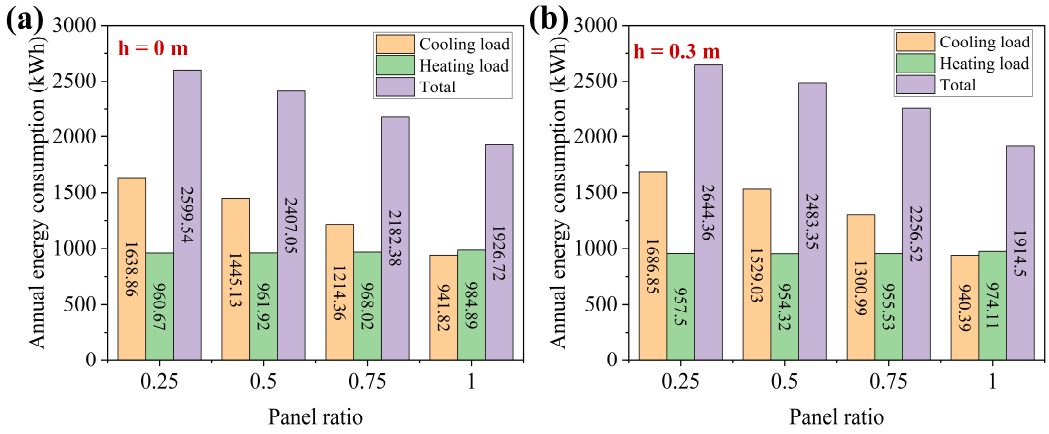


Figure 7. Annual HVAC energy consumption at panel-to-roof gaps of (**a**) h = 0 m and (**b**) h = 0.3 m for different roof coverage ratios.

Among the two geometric parameters considered above, the roof coverage ratio had a much greater influence on HVAC energy consumption. Regardless of the panel-to-roof gap, increasing the RC coverage ratio consistently reduced the annual HVAC load. As shown in Figure 7, this trend was particularly pronounced at h = 0.3 m; when the coverage ratio was increased from 25% to 100%, the total load decreased from 2644.4 kWh to 1914.5 kWh. This reduction was attributable almost entirely to the decrease in cooling load. Specifically, the cooling load decreased from 1686.9 kWh to 940.4 kWh, whereas the heating load increased slightly from 957.5 kWh to 974.1 kWh. In other words, increasing RC roof coverage significantly improved cooling-season performance while imposing only a relatively small additional heating burden under adaptive operation.

Based on these parametric results, the performance of the adaptive RC panel was governed primarily by the roof coverage ratio, whereas the panel-to-roof gap had a comparatively minor influence. This observation is consistent with previous studies showing that roof-mounted shading systems can substantially reduce roof heat gain and building cooling demand [46]. In the present study, full roof coverage reduced annual HVAC energy consumption by approximately 30.7% compared with that of the baseline roof. Once full coverage is achieved, the panel-to-roof gap may therefore be selected mainly according to practical design requirements rather than marginal differences in energy savings. Furthermore, structural support, roof drainage, maintenance access, and installation feasibility should be considered more important design constraints than the relatively small variations in simulated HVAC load associated with changes in the panel-to-roof gap.

3.4. Energy Performance Assessment of Different Roof Configurations across Nine Representative Chinese Cities

To determine the climatic suitability of the RC panel across China, its performance was evaluated in representative cities under different climatic conditions. Three roof configurations were compared in each city: the baseline roof, the fixed RC panel, and the adaptive RC panel. Figure 8 shows the monthly cooling, heating, and total HVAC loads for the three roof configurations in the selected cities.

The baseline-roof cases provide a reference for examining the influence of climatic conditions on building energy demand without the effects of RC. Harbin, Urumqi, Yinchuan, and Beijing are northern cities characterized by substantial winter heating demand, resulting in relatively high annual HVAC energy consumption. In January, the heating loads of these four cities were 804.7, 737.3, 555.7, and 603.7 kWh, respectively. In contrast, cooling demand was confined to a relatively short period, occurring primarily from June to August, with the peak generally occurring in July. Moving toward warmer climates, the HVAC load pattern shifted progressively from heating dominance to cooling dominance. Wuhan, Changsha, Kunming, Guangzhou, and Haikou are all in southern China and have relatively long cooling seasons with relatively low heating demand. In these southern cities, summer HVAC loads generally exceeded winter loads. Overall, the seasonal characteristics of energy demand varied substantially across regions: heating demand dominated winter energy consumption in northern China, whereas cooling demand dominated summer energy consumption in southern China.

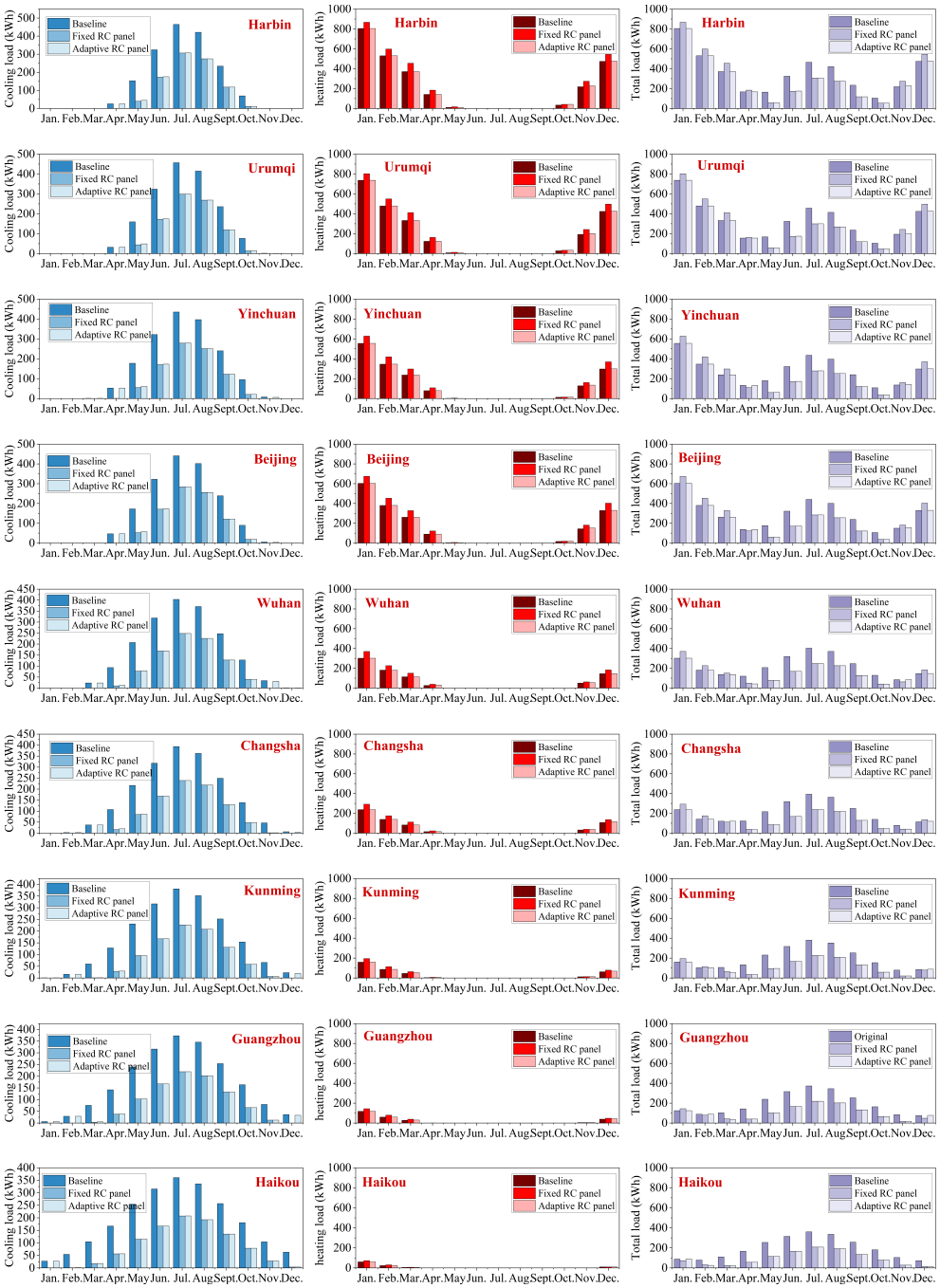


Figure 8. Monthly HVAC electricity consumption in nine representative cities—Harbin, Urumqi, Yinchuan, Beijing, Wuhan, Changsha, Kunming, Guangzhou, and Haikou—under the three roof configurations.

A fixed RC panel reduced cooling loads in all cities during summer. However, because the fixed panel remained in place throughout the year, it continued to provide radiative cooling during winter, when beneficial heat gains were needed. This increased heating demand during winter. Harbin, Urumqi, Yinchuan, and Beijing are representative cases in which the fixed panel reduced the summer cooling load but increased the winter heating load. In some winter months, the total HVAC load of the fixed-panel case was even higher than that of the baseline-roof case. Therefore, a fixed RC panel can achieve substantial cooling benefits but may be less suitable for cities with high winter heating demand.

The adaptive RC panel is a climate-responsive system that adjusts its operating period according to seasonal cooling and heating requirements. In Harbin, Urumqi, Yinchuan, and Beijing, the panel was operated mainly from May to October and removed during the primary heating season. In cities with milder winters, the panel remained in operation for a longer period. The panel was operated from April to October in Wuhan and from April to November in Changsha. In Kunming and Guangzhou, the panel was operated from March to November, whereas in Haikou it remained in operation for nearly the entire year, from February to December. The gradual extension of the operating period from northern to southern cities was consistent with increasing cooling demand in warmer climates.

During cooling-dominated months, the adaptive panel retained nearly the same cooling-load reduction as the fixed panel while avoiding the heating penalty associated with RC during heating-dominated months. Consequently, winter heating loads remained close to those of the baseline roof, whereas the fixed-panel case showed substantial increases. Beijing, Yinchuan, Wuhan, and Changsha are representative cities with substantial cooling demand in summer and heating demand in winter, making adaptive operation particularly beneficial. In the warmer cities of Guangzhou and Haikou, the difference between fixed and adaptive operation was relatively small because the heating season is short and cooling demand is high for most of the year.

Based on the monthly results, annual energy savings from the RC panel were calculated for the different climates. Figure 9 shows the annual energy savings of the fixed and adaptive RC panels for all representative cities. Both RC configurations reduced annual HVAC energy consumption in every city compared with the baseline roof, indicating that RC provided net annual energy savings in all selected climate zones.

However, the magnitude of the energy savings varied considerably among cities. Annual savings from the fixed RC panel were relatively small in cold cities such as Harbin, Urumqi, Yinchuan, and Beijing but were more substantial in warmer cities. This pattern reflects the different balance between cooling and heating demand across climates. Although a fixed panel can reduce summer cooling demand in cold climates, its continued operation during winter increases heating demand. Therefore, part of the cooling benefit is offset by increased heating energy consumption. As the climate becomes warmer and the heating season shorter, this offsetting effect becomes less significant, allowing the cooling advantage of a fixed panel to contribute more directly to annual energy savings.

The adaptive RC panel achieved better annual performance by addressing this seasonal imbalance. Because the panel operated mainly during cooling-dominated periods and additional radiative cooling was avoided during heating-dominated months, most of the cooling benefit was retained while the winter heating penalty was minimized. Therefore, the adaptive configuration achieved greater annual energy savings than the fixed configuration in most cities. The advantage of adaptive operation was particularly evident in climates with substantial seasonal contrasts between summer cooling and winter heating demand.

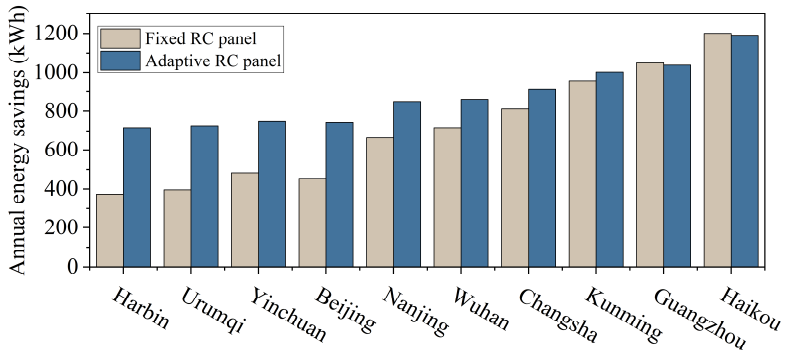


Figure 9. Annual HVAC energy savings under the fixed and adaptive RC panel configurations.

A direct comparison showed that adaptive operation generally outperformed fixed-panel operation. Figure 10 shows the additional annual energy savings achieved by the adaptive panel relative to the fixed panel, which were highly climate-dependent. The additional savings were greatest in cities with long or severe winters. Harbin

showed the greatest improvement, with the adaptive panel saving 343.85 kWh more than the fixed panel, followed by Urumqi (331.02 kWh), Beijing (289.23 kWh), and Yinchuan (266.82 kWh). In these cities, severe winter conditions make year-round use of the RC panel less desirable because it limits beneficial solar heat gains and increases heating demand. By removing the panel during the heating season, adaptive operation reduced total annual HVAC energy consumption.

Adaptive operation also retained an advantage in hot-summer and cold-winter cities, although the magnitude of this advantage was smaller than in colder northern cities. Compared with the fixed panel, the adaptive panel reduced annual HVAC energy consumption by 184.98 kWh in Nanjing, 143.38 kWh in Wuhan, and 99.14 kWh in Changsha. These cities experience high cooling demand during summer while retaining substantial heating demand in winter. Although the fixed panel provided substantial cooling benefits during summer, it also imposed an additional heating penalty during winter. In such mixed-demand climates, the adaptive strategy avoids unfavorable winter effects by removing the panel during heating-dominated periods.

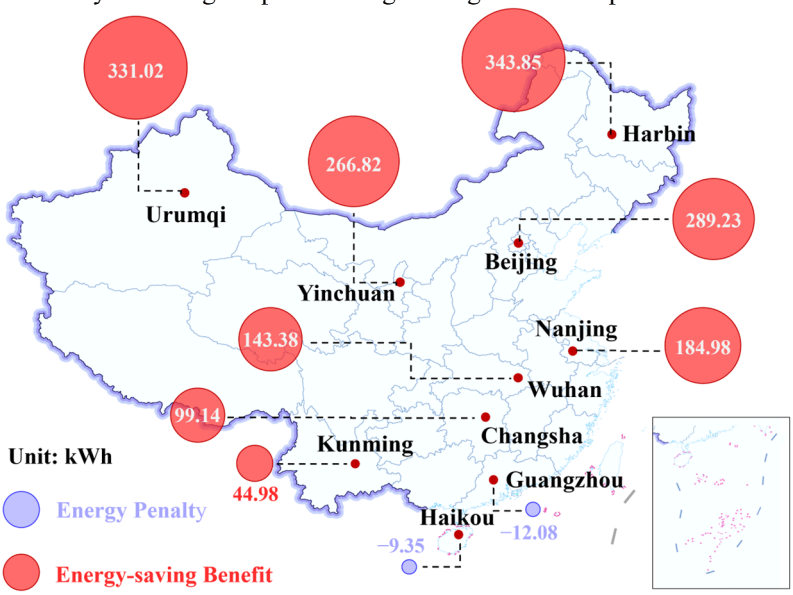


Figure 10. Additional annual HVAC energy savings achieved by the adaptive RC strategy relative to the fixed RC panel.

In contrast, the additional benefit of adaptive operation decreased markedly in cooling-dominated climates. In Kunming, the energy saving of adaptive approach was 44.98 kWh, while in Guangzhou and Haikou, the difference between the two strategies became negligible. As heating demand weakens and the cooling season extends, the penalty associated with fixed installation becomes progressively smaller, and the need for panel removal is correspondingly reduced. In Haikou, where cooling dominates almost year-round, the fixed panel was even marginally more advantageous than the adaptive strategy, indicating that continuous installation was already close to the local optimum.

4. Discussion

The results demonstrate that RC technologies should not be selected solely on the basis of idealized or peak cooling performance. High solar reflectance and high mid-infrared emittance reduce roof heat gain during hot periods, but suppress beneficial solar heat gains in winter. The more appropriate performance metric is therefore net annual HVAC energy consumption, accompanied by separate reporting of cooling-energy savings and heating-energy penalties [47,48].

This seasonal trade-off is particularly important for large-scale deployment. Fixed RC roofs may be suitable for strongly cooling-dominated climates, where winter heating demand is limited and the additional benefit of seasonal control may be small. In heating-dominated and mixed climates, a permanently exposed RC surface can reduce summer cooling demand but increase winter heating demand. Climate classification alone is therefore insufficient; seasonal building-load balance should also be incorporated into design guidance and performance standards [49].

As shown in Figure 11, the adaptive panel offers a practical means of introducing seasonal control without relying on intrinsically switchable materials. The panel can be deployed above the roof during cooling-dominated periods and retracted, repositioned, or otherwise deactivated during heating-dominated periods. In this way, the roof

functions as a climate-responsive envelope system rather than as a surface with permanently fixed optical and radiative properties.

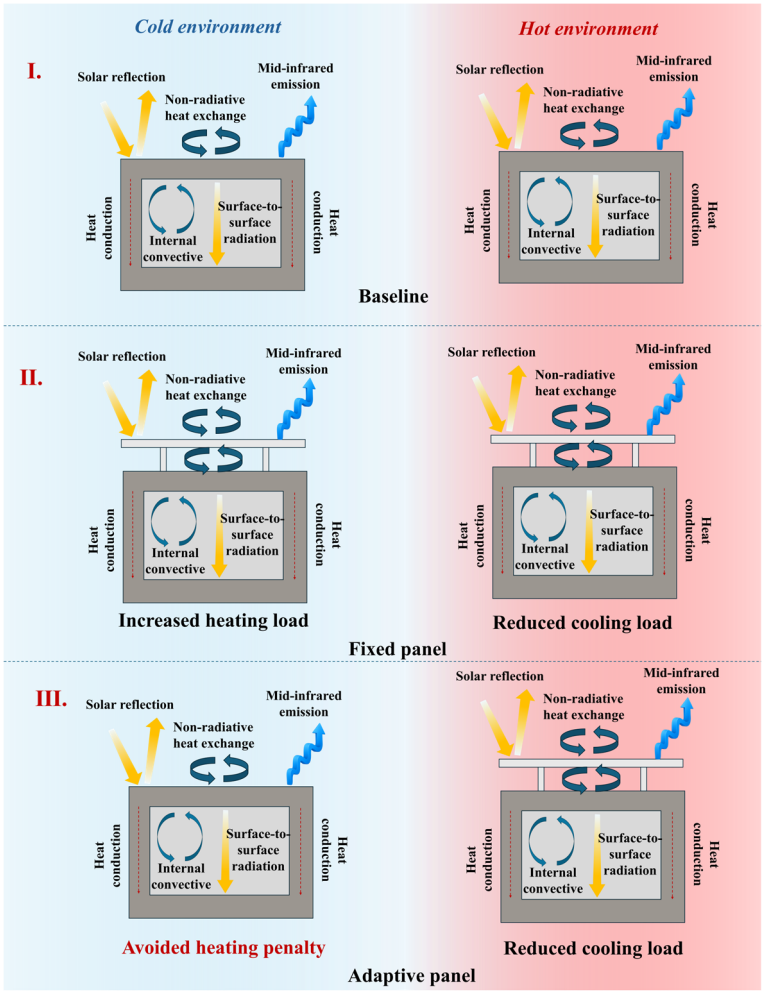


Figure 11. Schematic of the three roof configurations under cooling- and heating-dominated conditions.

The benefit of this adaptive strategy varies across climate zones. In heating-dominated and mixed climates, its principal value lies in avoiding excessive radiative heat rejection during winter. In hot-summer–cold-winter regions, seasonal operation can address the opposing requirements of summer heat rejection and winter heat retention. By contrast, in strongly cooling-dominated climates, fixed installation may already provide most of the attainable annual energy benefit, making the incremental advantage of movability relatively limited.

Accordingly, RC systems should be evaluated by considering not only material optical properties but also local weather conditions, monthly heating and cooling loads, building characteristics, operating schedules, control strategies, and practical installation constraints. RC roofs should therefore be regarded as climate-responsive building-envelope systems rather than universally applicable cooling solutions. A design that minimizes roof heat gain in summer does not necessarily achieve the lowest annual HVAC energy consumption, particularly when seasonal control is unavailable. The proposed movable panel may broaden the applicability of RC in climates with substantial heating demand, provided that its operation is informed by climate-zone characteristics, building-load profiles, and clearly defined seasonal control strategies.

The adaptive strategy considered in this study should be interpreted as an offline, load-based monthly scheduling method rather than a real-time or forecast-based controller. The installation schedule was determined retrospectively from the monthly cooling and heating demands of the baseline-roof case using the complete annual weather dataset. Consequently, the reported savings represent an idealized performance estimate for the proposed monthly scheduling framework, assuming perfect knowledge of baseline loads and neglecting forecast errors, control delays, switching constraints, and the energy required to operate the installation mechanism.

The present analysis also excludes actuator energy consumption, installation and switching mechanisms, wind resistance, structural safety, mechanical fatigue, material degradation, maintenance requirements, and life-

cycle costs. Therefore, the results quantify the potential building-level thermal and HVAC energy benefits of seasonal radiative-cooling adaptation, rather than the net performance of a fully implemented control system.

Future work will focus on developing and experimentally validating an implementable adaptive system. This will include forecast-based or model-predictive control using short-term weather and building-load predictions, real-time temperature feedback, switching hysteresis, minimum dwell times, and operational constraints under extreme weather conditions. The energy consumption, reliability, wind resistance, durability, maintenance requirements, and life-cycle economics of the switching mechanism will also be evaluated. Passive temperature-responsive coatings and mechanically adaptive radiative switches demonstrated in previous studies provide promising pathways for the practical realization of such systems.

Another limitation of this study is that the cross-city analysis was based on a single standardized reference building. This approach was adopted to control building geometry, window-to-wall ratio, internal heat gains, thermal mass, and HVAC parameters, thereby isolating the influence of climatic conditions on the relative performance of the different roof configurations. Consequently, the results represent the conditional performance of the reference building under the meteorological conditions of the selected cities and cannot be directly generalized to all building types. Because the contribution of the roof to the total building load varies with the roof-to-building area ratio, window-to-wall ratio, internal heat gains, and thermal mass, the magnitude of energy savings may differ for other building archetypes. Future research will incorporate building archetypes with different scales, functions, and thermal characteristics to further evaluate the generalizability and robustness of the proposed strategy.

5. Conclusions

This study investigates whether an adaptive radiative cooling (RC) panel can overcome the seasonal trade-off of conventional RC roofs by maintaining cooling benefits during warm periods while avoiding heating penalties during cold periods across different climates. A transient thermodynamic model was developed to evaluate the thermal and energy performance of the different roof configurations under multiple Chinese climatic conditions.

The performance and energy-saving potential of the RC panel were strongly influenced by seasonal cooling and heating demands. For the baseline-roof case in Nanjing, annual HVAC energy consumption was 2763.8 kWh, of which 65.2% was attributed to cooling, indicating that cooling dominated annual energy use. Nevertheless, winter heating demand remained substantial. Continuous year-round application of RC could therefore reduce cooling energy use during warm periods but increase heating demand during cold periods. The free-floating indoor-temperature results further confirmed this seasonal trade-off. These findings show that the benefits of RC depend on when cooling is required and support the use of an adaptive rather than a permanently installed RC configuration.

Both RC panel configurations (fixed and adaptive) reduced annual HVAC electricity consumption, but adaptive RC operation performed better. In Nanjing, the fixed RC panel reduced annual consumption to 2099.5 kWh, representing savings of 24.0%, whereas the adaptive panel reduced it to 1914.5 kWh, representing savings of 30.7%. The difference arose primarily because adaptive operation retained the baseline roof during heating-dominated months and thereby avoided most of the winter penalty.

Panel coverage had a substantially greater influence on annual performance than panel-to-roof spacing. Once full coverage was achieved, changes in spacing produced only minor differences in simulated annual consumption, suggesting that spacing should be selected primarily on the basis of structural support, drainage, ventilation, maintenance access, and constructability. Across the selected cities, adaptive RC deployment provided the largest incremental benefit in cold and mixed climates, including Harbin, Urumqi, Beijing, and Yinchuan. By contrast, its advantage was small in strongly cooling-dominated cities such as Guangzhou and Haikou. These findings support climate-specific deployment rather than uniform year-round application.

Future work will focus on experimental validation of the proposed adaptive RC roof under real-world weather conditions. More detailed control strategies based on short-term weather forecasts and actual indoor thermal demand should also be investigated to replace the current monthly switching approach. In addition, the effects of different building types, roof constructions, installation mechanisms, long-term durability, and life-cycle costs should be evaluated to support the practical design and large-scale application of adaptive RC systems.

Author Contributions

Y.H.: Conceptualization, Methodology, Investigation, Formal Analysis, Writing—Original Draft. B.Z.: Conceptualization, Investigation, Writing—Review and Editing. Y.Z.: Conceptualization, Investigation. W.M.: Conceptualization, Investigation, Writing—Review and Editing. All authors have read and agreed to the published version of the manuscript.

Funding

This research was funded by the Postgraduate Research & Practice Innovation Program of Jiangsu Province (No. KYCX25 0428) and the SEU Innovation Capability Enhancement Plan for Doctoral Students (No. CXJH SEU 25100).

Institutional Review Board Statement

Not applicable.

Informed Consent Statement

Not applicable.

Data Availability Statement

Data are available from the corresponding authors upon reasonable request.

Acknowledgments

The authors gratefully acknowledge financial support from the Postgraduate Research & Practice Innovation Program of Jiangsu Province (No. KYCX25 0428) and the SEU Innovation Capability Enhancement Plan for Doctoral Students (No. CXJH_SEU 25100).

Conflicts of Interest

The authors declare no conflict of interest.

Use of AI and AI-Assisted Technologies

No AI tools were utilized for this paper.

References

1. Zhong, X.; Voogt, J.; Zhan, W.; et al. UAV-based low-altitude remote sensing in built-environment thermal studies: A review across different spatial scales. *Build. Environ.* **2026**, *303*, 114937.
2. Wang, D.; Zhou, Y.; Zheng, X.; et al. Optimizing Urban Morphology for Net-Zero Energy Districts: A Data-Driven Planning Framework. *Energy Use* **2026**, *2*, 100040.
3. Santamouris, M. Cooling the cities—A review of reflective and green roof mitigation technologies to fight heat island and improve comfort in urban environments. *Sol. Energy* **2014**, *103*, 682–703.
4. Hughes, B.R.; Chaudhry, H.N.; Ghani, S.A. A review of sustainable cooling technologies in buildings. *Renew. Sustain. Energy Rev.* **2011**, *15*, 3112–3120.
5. Leo Samuel, D.G.; Shiva Nagendra, S.M.; Maiya, M.P. Passive alternatives to mechanical air conditioning of building: A review. *Build. Environ.* **2013**, *66*, 54–64.
6. Oropeza-Perez, I.; Østergaard, P.A. Active and passive cooling methods for dwellings: A review. *Renew. Sustain. Energy Rev.* **2018**, *82*, 531–544.
7. Akbari, H.; Menon, S.; Rosenfeld, A. Global cooling: Increasing world-wide urban albedos to offset CO_2. *Clim. Change* **2009**, *94*, 275–286.
8. Synnefa, A.; Santamouris, M.; Akbari, H. Estimating the effect of using cool coatings on energy loads and thermal comfort in residential buildings in various climatic conditions. *Energy Build.* **2007**, *39*, 1167–1174.
9. Pisello, A.L. State of the art on the development of cool coatings for buildings and cities. *Sol. Energy* **2017**, *144*, 660–680.
10. Raman, A.P.; Anoma, M.A.; Zhu, L.; et al. Passive radiative cooling below ambient air temperature under direct sunlight. *Nature* **2014**, *515*, 540–544.
11. Rephaeli, E.; Raman, A.; Fan, S. Ultrabroadband Photonic Structures To Achieve High-Performance Daytime Radiative Cooling. *Nano Lett.* **2013**, *13*, 1457–1461.
12. Gentle, A.R.; Smith, G.B. Radiative Heat Pumping from the Earth Using Surface Phonon Resonant Nanoparticles. *Nano Lett.* **2010**, *10*, 373–379.
13. Mandal, J.; Fu, Y.; Overvig, A.C.; et al. Hierarchically porous polymer coatings for highly efficient passive daytime radiative cooling. *Science* **2018**, *362*, 315–319.
14. Li, X.; Peoples, J.; Huang, Z.; et al. Full daytime sub-ambient radiative cooling in commercial-like paints with high figure of merit. *Cell Rep. Phys. Sci.* **2020**, *1*, 100221.

15. Li, X.; Peoples, J.; Yao, P.; et al. Ultrawhite $BaSO_4$ paints and films for remarkable daytime subambient radiative cooling. *ACS Appl. Mater. Interfaces* **2021**, *13*, 21733–21739.
16. Zhao, B.; Hu, M.; Ao, X.; et al. Radiative cooling: A review of fundamentals, materials, applications, and prospects. *Appl. Energy* **2019**, *236*, 489–513.
17. Fan, S.; Li, W. Photonics and thermodynamics concepts in radiative cooling. *Nat. Photonics* **2022**, *16*, 182–190.
18. Munday, J.N. Tackling climate change through radiative cooling. *Joule* **2019**, *3*, 2057–2060.
19. Liang, J.; Wu, J.; Guo, J.; et al. Radiative cooling for passive thermal management towards sustainable carbon neutrality. *Natl. Sci. Rev.* **2023**, *10*, nwac208.
20. Kousis, I.; D'Amato, R.; Pisello, A.L.; et al. Daytime Radiative Cooling: A Perspective toward Urban Heat Island Mitigation. *ACS Energy Lett.* **2023**, *8*, 3239–3250.
21. Anand, J.; Sailor, D.J.; Baniassadi, A. The relative role of solar reflectance and thermal emittance for passive daytime radiative cooling technologies applied to rooftops. *Sustain. Cities Soc.* **2021**, *65*, 102612.
22. Pirvaram, A.; Talebzadeh, N.; Leung, S.N.; et al. Radiative cooling for buildings: A review of techno-enviro-economics and life-cycle assessment methods. *Renew. Sustain. Energy Rev.* **2022**, *162*, 112415.
23. Zeyghami, M.; Goswami, D.Y.; Stefanakos, E. A review of clear sky radiative cooling developments and applications in renewable power systems and passive building cooling. *Sol. Energy Mater. Sol. Cells* **2018**, *178*, 115–128.
24. Zhang, K.; Zhao, D.; Yin, X.; et al. Energy saving and economic analysis of a new hybrid radiative cooling system for single-family houses in the USA. *Appl. Energy* **2018**, *224*, 371–381.
25. Peoples, J.; Hung, Y.-W.; Fang, Z.; et al. Energy savings of radiative cooling paints applied to residential buildings. *Int. J. Heat Mass Transf.* **2022**, *194*, 123001.
26. Zhang, W.; Jiao, D.; Zhao, B.; et al. Experimental and numerical investigation of the effects of passive radiative cooling-based cool roof on building energy consumption. *Appl. Energy* **2024**, *376*, 124161.
27. Bu, F.; Yan, D.; Tan, G.; et al. Systematically incorporating spectrum-selective radiative cooling into building performance simulation: Numerical integration method and experimental validation. *Appl. Energy* **2022**, *312*, 118733.
28. Li, X.; Sun, B.; Sui, C.; et al. Integration of daytime radiative cooling and solar heating for year-round energy saving in buildings. *Nat. Commun.* **2020**, *11*, 6101.
29. Tang, K.; Dong, K.; Li, J.; et al. Temperature-adaptive radiative coating for all-season household thermal regulation. *Science* **2021**, *374*, 1504–1509.
30. An, Y.; Fu, Y.; Dai, J.-G.; et al. Switchable radiative cooling technologies for smart thermal management. *Cell Rep. Phys. Sci.* **2022**, *3*, 101098.
31. Zhao, X.; Li, J.; Dong, K.; et al. Switchable and Tunable Radiative Cooling: Mechanisms, Applications, and Perspectives. *ACS Nano* **2024**, *18*, 18118−18128.
32. Sui, C.; Pu, J.; Chen, T.; et al. Dynamic electrochromism for all-season radiative thermoregulation. *Nat. Sustain.* **2023**, *6*, 428–437.
33. Zhang, H.; Huang, J.; Fan, D. Switchable radiative cooling from temperature-responsive thermal resistance modulation. *ACS Appl. Energy Mater.* **2022**, *5*, 6003–6010.
34. Kommandur, S.; Kishore, R. A. Contact-Based Passive Thermal Switch with a High Rectification Ratio. *ACS Eng. Au* **2023**, *3*, 76–83.
35. Hersbach, H.*;* Bell, B.; Berrisford, P.; et al. *ERA5 Hourly Data on Single Levels from 1940 to Present*; Copernicus Climate Change Service (C3S) Climate Data Store (CDS), 2023. Available online: https://climatereanalyzer.org/clim/t2_daily/ (accessed on 5 April 2026).
36. Hu, Y.; Guo, T.; Qu, X.; et al. Replaceable cement-based radiative cooling panels for buildings: Thermal and economic superiority over coatings. *J. Build. Eng.* **2026**, *121*, 115634.
37. Fuentes, M.K. *A Simplified Thermal Model for Flat-Plate Photovoltaic Arrays*; Sandia National Labs: Albuquerque, NM, USA, 1987.
38. Fabiani, C.; Pisello, A.L.; Bou-Zeid, E.; et al. Adaptive measures for mitigating urban heat islands: The potential of thermochromic materials to control roofing energy balance. *Appl. Energy* **2019**, *247*, 155–170.
39. Palyvos, J.A. A survey of wind convection coefficient correlations for building envelope energy systems' modeling. *Appl. Therm. Eng.* **2008**, *28*, 801–808.
40. Hu, Y.; Guo, T.; Qu, X.; et al. Enhanced passive radiative cooling of cementitious composites for efficient photovoltaic thermal management. *Energy Convers. Manag.* **2025**, *344*, 120268.
41. Chen, Z.; Wen, J.; Bushby, S.T.; et al. An Analysis of the Hybrid Internal Mass Modeling Approach in EnergyPlus. In Proceedings of the 12th eSim Building Simulation Conference, Ottawa, ON, Canada, 22–23 June 2022.
42. Carlos, J.S.; Corvacho, H. Evaluation of the performance indices of a ventilated double window through experimental and analytical procedures: SHGC-values. *Energy Build.* **2015**, *86*, 886–897.

43. Hoyt, T.; Arens, E.; Zhang, H. Extending air temperature setpoints: Simulated energy savings and design considerations for new and retrofit buildings. *Build. Environ.* **2015**, *88*, 89–96.
44. Hu, Y.; Shen, B. Development and field demonstration of residential air source integrated heat pump using a three-stage compressor. *Energy Build.* **2025**, *328*, 115202.
45. Wijesuriya, S.; Kishore, R.A.; Bianchi, M.V.A.; et al. Potential energy savings benefits and limitations of radiative cooling coatings for U.S. residential buildings. *J. Clean. Prod.* **2022**, *379*, 134763.
46. Bhuvad, S.S. Investigation of annual performance of a building shaded by rooftop PV panels in different climate zones of India. *Renew. Energy* **2022**, *189*, 1337–1357.
47. An, J.; Li, H.; Bu, F.; et al. A systematic analysis of energy-saving potential of spectrum-selective radiative cooling materials in buildings. *J. Build. Eng.* **2024**, *91*, 109620.
48. Yang, Y.; Zhang, G.; Rong, L. Temperature adaptive passive daytime radiative cooling: The impact of their essential properties on energy performance of different building types. *Energy Build.* **2024**, *325*, 114955.
49. Yazdani, H.; Baneshi, M. Building energy comparison for dynamic cool roofs and green roofs under various climates. *Sol. Energy* **2021**, *230*, 764–778.